

PETROPHYSICAL ANALYSIS OF WELL MANZALAI-01 UPPER INDUS BASIN, PAKISTAN



A thesis submitted to Bahria University, Islamabad in partial fulfillment of
the requirement for the degree of BS in Geology

**ABDUL RAFAY MALIK
MUHAMMAD HAMZA TARIQ
SABAHAT FATIMA**



**Department of Earth and Environmental Sciences
Bahria University Islamabad Campus**




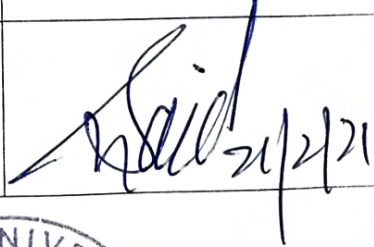
2020

Bahria University
Department of Earth & Environmental Sciences
Islamabad Campus, Islamabad

Dated: 16/02/2021

Certificate

This thesis is submitted by **Ms. Sabahat Fatima, Mr. Muhammad Hamza Tariq and Mr. Abdul Rafay Malik** is accepted in the present form by Department of Earth & Environmental Sciences, Bahria University, Islamabad as the partial fulfillment of the requirement for the degree of **Bachelor of Sciences in Geology**, 4 years program (Session 2017 – 2020).

Committee Members	Name	Signature
Supervisor	Mr. Saqib Mehmood	
Internal Examiner	Dr. Muhsan Ehsan	
External Examiner	Dr. Saiq Shakeel Abbasi	
Head of Department (E&ES)	Dr. Said Akbar Khan	



ABSTRACT

The objective of this research is to determine the hydrocarbon potential of well Manzalai-01. The well Manzalai-01 is located in the western part of the Upper Indus Basin. Tectonically, the respective well is located in the Kohat sub Basin near Kurram fault. The tectonic regime of this area is compressional where both strike slip and thrust faults are present. For petro-physical analysis, log data for well Manzalai-01 was acquired from LMKR approved by DGPC, Islamabad. In well Manzalai-01, two zones of interests have been identified on the basis of logs trends. One prospect zone has been marked in Lockhart Limestone and one zone of interest has been marked in the Lumshiwai Formation. The various petro-physical parameters were calculated for Lockhart Formation and Lumshiwai Formation. Petro-physical Analysis suggests that average volume of shale Average Percentage is 13% for prospect zone of Lockhart Formation and 14.33% for prospect zone of Lumshiwai Formation. Average porosity for prospect zone of Lockhart Formation is 2.71% and for prospect zone of Lumshiwai Formation is 2.38% Average effective porosity for prospect zone of Lockhart Formation is 2.35% and for prospect zone of Lumshiwai Formation 2.06% , the average water saturation is 5.2% and 52.1% , the average hydrocarbon potential is 94.7% and 47.83% for Lockhart and Lumshiwai formations respectively. The results showed that in well Manzalai-01, both clastic and carbonate reservoirs are present. On the basis of low percentage of volume of shale and the high percentage of the hydrocarbons, the results computed that both formations are acting as major reservoirs in well Manzalai-01.

ACKNOWLEDGEMENTS

First of all bowing our head to Allah Almighty, the most powerful and the most gracious. Allah made us capable of successfully completing this research work. Immense salutations are upon Holy Prophet Muhammad (P.B.U.H), the basis of wisdom who always directed His Ummah to seek knowledge. After that, we are thankful to our beloved parents for strengthening us in order to achieve our goal with their best wishes, prayers, and kindness. We are obligated to our Honorable Supervisor Mr. Saqib Mehmood, Senior Assistant Professor, Department of Earth and Environmental Sciences, Bahria University Islamabad Campus for their professional guidance, ongoing support and devotion throughout our research work.

The words of thanks go to Prof. Dr. Said Akbar Khan, Head of Department, Department of Earth and Environmental Sciences, Bahria University Islamabad Campus for his encouragement and concern. We are also grateful to Mr. Adeeb Ahmed, and all the other esteemed teachers for their assistance and cooperation with us in conducting this research.

CONTENTS

	Page
ABSTRACT	i
ACKNOWLEDGEMENT	ii
FIGURES	vi
TABLES	vii
ABBREVIATION	viii

CHAPTER 1

INTRODUCTION

1.1	General Introduction	1
1.2	Exploration history	2
1.3	Location	3
1.4	Objectives	3
1.5	Methodology	3

CHAPTER 2

TECTONICS AND STRATIGRAPHY

2.1	Tectonics	5
2.2	Generalized stratigraphy of Upper Indus Basin	7
2.3	Borehole well stratigraphy	8
2.4	Petroleum play	9

CHAPTER 3

PETRO-PHYSICAL ANALYSIS

3.1	Introduction	10
3.2	Steps for petro-physical analysis	10
3.3	Methodology	10
3.3.1	Zone of interest	11
3.3.2	Calculation of volume of shale	11
3.3.3	Volume of clean	12

3.3.4	Porosity analysis and calculations	12
3.3.4.1	Density porosity	12
3.3.4.2	Neutron porosity	13
3.3.4.3	Sonic porosity	13
3.3.4.4	Average porosity	13
3.3.4.5	Effective porosity	13
3.3.4.6	Resistivity of water	14
3.3.4.7	Water saturation	15
3.3.4.8	Hydrocarbon saturation	15
3.4	Petro-physical interpretation of well Manzalai-01	16
3.4.1	Zone of interest	16
3.4.2	Petro-physical analysis of Lockhart formation in well Manzalai-01	16
3.4.2.1	Volume of shale (Vsh) of zone of interest within Lockhart formation	18
3.4.2.2	Calculation of porosities of zone of interest within Lockhart formation	18
I.	Neutron porosity	18
II.	Density porosity	19
III.	Sonic porosity	19
IV.	Average porosity	19
V.	Effective porosity	20
3.4.2.3	Relationship between Vshale and porosities	20
3.4.2.4	Resistivity of water of zone of interest	21
3.4.2.5	Saturation of water and saturation of hydrocarbon in zone of interest	26
3.4.2.6	Results	27
3.4.3	Petro-physical analysis of Lumshiwai formation in well Manzalai-01	27
3.4.3.1	Volume of shale (Vsh) of zone of interest within Lumshiwai formation	29
3.4.3.2	Calculation of porosities of zone of interest within Lumshiwai formation	30
I.	Neutron porosity	30
II.	Density porosity	30
III.	Sonic porosity	30
IV.	Average porosity	31
V.	Effective porosity	31

3.4.3.3	Relationship between Vshale and porosities	31
3.4.3.4	Resistivity of water of zone of interest	32
3.4.3.5	Saturation of water and saturation of hydrocarbon of zone of interest	37
3.4.3.6	Results	39
	CONCLUSION	40
	REFERENCES	41
	APPENDIX	42

FIGURES

		Page
Figure 1.1	Location map of study area.	3
Figure 2.1	Tectonic map of study area.	6
Figure 2.2	Generalized stratigraphy of Upper Indus Basin, Pakistan.	7
Figure 3.1	Log trends of Zone A, marked within Lockhart formation.	17
Figure 3.2	Relationship between volume of shale and volume of clean.	18
Figure 3.3	Variation in Φ_{iS} , Φ_{iA} and Φ_{iE} .	21
Figure 3.4	Gen-9 for conversion of R_{mf} from surface temperature to formation temperature.	23
Figure 3.5	SP-2 for conversion of R_{mf} to $R_{mf_{eq}}$.	24
Figure 3.6	SP-1 for conversion of $R_{mf_{eq}}$ to R_{weq} .	25
Figure 3.7	Variation in water saturation and hydrocarbon saturation within marked zone of interest.	26
Figure 3.8	Log trends of Zone B, marked within Lumshiwai Formation.	28
Figure 3.9	Relationship between V_{shale} and V_{clean} .	29
Figure 3.10	Relationship between V_{shale} and porosities.	32
Figure 3.11	Gen-9 for conversion of R_{mf} from surface temperature to formation temperature.	34
Figure 3.12	SP-2 for conversion of R_{mf} to $R_{mf_{eq}}$.	35
Figure 3.13	SP-1 for conversion of $R_{mf_{eq}}$ to R_{weq} .	36
Figure 3.14	Variation in water saturation and hydrocarbon saturation within marked zone of interest.	38

TABLES

	Page
Table 2.1	8
Table 2.2	9
Table 3.1	16
Table 3.2	19
Table 3.3	19
Table 3.4	19
Table 3.5	20
Table 3.6	20
Table 3.7	27
Table 3.8	30
Table 3.9	30
Table 3.10	30
Table 3.11	31
Table 3.12	31
Table 3.13	39

ABBREVIATIONS

R _{mc}	Resistivity of Mud Cake
R _{mf}	Resistivity of Mud Filtrate
R _m	Resistivity of Mud
R _{xo}	Resistivity of Flushed Zone
R _t	Resistivity of True Zone
R _w	Resistivity of Water
R _{mfeq}	Equivalent Mud Filtrate Resistivity
R _{w_{eq}}	Equivalent Formation Water Resistivity
S _h	Saturation of Hydrocarbons
S _w	Saturation of Water
D _i	Diameter of Invaded Zone
D _h	Diameter of Borehole
G.G	Geothermal Gradient
S.T	Surface Temperature
B.H.T	Bottom Hole Temperature
SPDZ	South Potwar Deformed Zone
NPDZ	North Potwar Deformed Zone
MMBBL	Million Barrels Oil
MMCFD	Million Cubic Feet per Day
BOPL	Barrel of Oil per Day
BBO	Billion barrels of oil
TCF	Trillion cubic feet

CHAPTER 1

INTRODUCTION

1.1 General introduction

The Islamic Republic of Pakistan is located in the South East of Asia. Pakistan, the fifth most populated country on the planet with an evaluation of over 212.2 million population have more than 9 BBO as well as 105 TCF of natural gas reserves. (Saleh, 2015)

Almighty Allah has blessed Pakistan with a significant amount of oil and gas reserves, which assuredly are very crucial for the optimization, economy and providence for the financial growth of the country. Hydrocarbons play a vital role being the significant source of energy and economy. Ascertaining the Hydrocarbon content subsequent to its production is indeed very critical. These reserves are found under the suitable conditions into the sedimentary basins.

Pakistan has two Sedimentary basins:

1. Indus Basin.
2. Baluchistan Basin. (Ibrahim, 2009)

The study area, well Manzalai-01 is situated in the west of the Upper Indus Basin. The lithological columns of Tal block's Manzalai wells reflect a comprehensive depositional record of sedimentary accumulation from Jurassic to Palaeocene i.e, 200-55 million years. The eight formations can indeed be identified throughout the Manzalai wells with almost the same names as well as palaeo-facies, but often with a slightly distinct petrographic as well as sedimentary, palaeontological outline and varying sequence. (Berecz, 2010)

There are a number of oil and gas discoveries in the respective region. Indus basin is a massive basin and the drilling pursuits have been carried out in the respective area in the sub-continent as well. Pakistan, offers a promising prospects for exploring the

resources of oil and gas. Until that, nevertheless, the pursuits in the domain of exploration and production of hydrocarbon resources in the country have remained intermittent cyclical and chiefly depends on the feedback of the multinational companies in this sector. New avenues are arising through technological advancement.

Core Analysis, wire-line logging and mud logging are the most effective approaches for measuring and analyzing the formation's chemical and physical properties, providing information on rock types, the composition of the fluid present and several other aspects of petro-physics.

We therefore need to understand the lithology, permeability, porosity, density including saturation of water and/or other fluids present for petro-physical study (Mavko et al., 2003).

1.2 Exploration History

In December 2002, the hydrocarbon exploration activity was conducted in the Tal Block (KPK), which resulted in the discovery of the well Mazalai-01.

1.3 Location

The well Manzalai-01 is located at Tal Block of KPK at latitude 33°16'43" N and longitude 70°48'57.59" E as shown in figure 1.1.

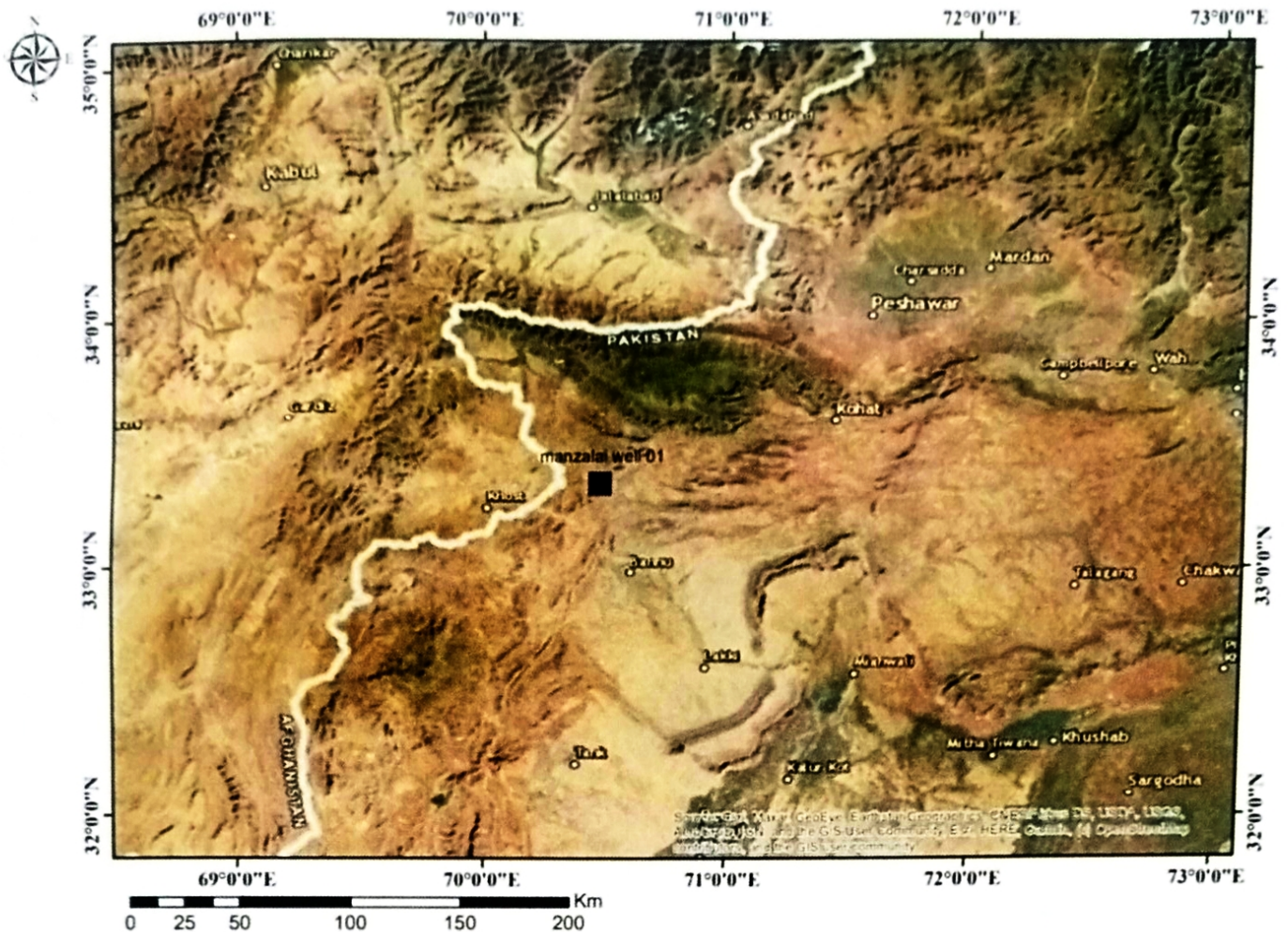


Figure 1.1: Location map of study area (ArcGIS)

1.4 Objectives

The well of interest i.e, well Manzalai-01 is located in the Tal block (KPK, Pakistan). In the Kohat sub-basin, various wells had been drilled already but not much information has been collected, assessed and evaluated for the benefit of the public. Nevertheless the related region has the capacity to carry out more exploration activities for oil and gas. The primary objective of this report was to investigate, formation evaluation of Manzalai 01 through petro-physical examination and the possible properties of multiple generating horizons of well Manzalai-01.

1.5 Methodology

- i. Mark the zone of interest
- ii. Estimation of volume of shale
- iii. Estimation of porosities
- iv. Estimation of Water Resistivity (R_w) by SP method

- v. Estimation of water saturation (S_w) by using Archie's equation
- vi. Calculation of Hydrocarbon saturation

Chapter 2

Tectonics and Stratigraphy

2.1 Tectonics

There was a collision between the Indian plate as well as the Eurasian plate around 55 to 50 million years ago that contributed to the uplifting of the Himalayas attributable to the geodynamic processes of continental drift from the southern hemisphere to the northern hemisphere, spreading of the sea floor including collision tectonics. The four fault systems, such as the Main Karakoram Thrust (MKT), Main Boundary Thrust (MBT) as well as the Salt Range Thrust, accompany the Kohat basin (SRT). The Karakoram block, the Kohistan Island arc, the Northern Deformed Fold-Thrust Belt, the Southern Deformed Fold and thrust Belt as well as the Punjab Fore deep divided the Pakistan Himalayas into different lithotectonic terrains between north of the Eurasian plate towards south of the Indian plate (Jan, 1997). The Surghar range, the southern Bannu basin as well as the northwestern Samana range establish the geographical boundaries of a Kohat plateau. The biggest centre on the Kohat plateau is now thought to be thrust and deformed to create the foreland geometry for the deposition of sediments that were mostly eroded during the Miocene. The first depocenter is the Kohat plateau. The southern boundary of the collision zone in North Pakistan is marked by the Kohat plateau and has well preserved Himalayan orogeny indentation. (Jan, 1997) In the early Miocene, the folding and thrusting belt of the Kohat foreland was found to be significant, and is also characteristic of sedimentary rocks ranging from paleocene to pliocene in ages. The oldest rocks exposed throughout the Kohat sub-basin containing Hangu, Lockhart limestone as well as Patala formation of paleocene age. (Jan, 1997) All such formations became accumulated either by Indian Plate margin loading throughout the fore-deep marine environment and represent the first known convergence of the Himalayas. The progression of the Paleocene is conformably overlain by the succession of Eocene (formations of Panoba, Jatta gypsum, Bahadurkhel Salt, Kuldana as well as Kohat (clastic and non-clastic rocks) accumulated in the small marine basins and denote a tectonically divided portion of Tethys seen between

continental margin with northwest India as well as the frontier of southern Asia. (Jan, 1997) The continuation of the Eocene is unconformably overlaid by either a dense succession of Miocene to the Murree, Kamliak as well as Siwalik group of Himalayan molasses. The northern section of the Kohat plateau spanning east-west is characterised by the Kohat range which contain jurassic to paleocene carbonates, shale, sandstone, including Datta, Shinawari, Samana Suk, Chichali, Lumshiwai, Kawagarh, Hangu, Lockhart limestone as well as Patala formation with a thickness of approximately 1300 metres mostly in proximity of TAL Block.

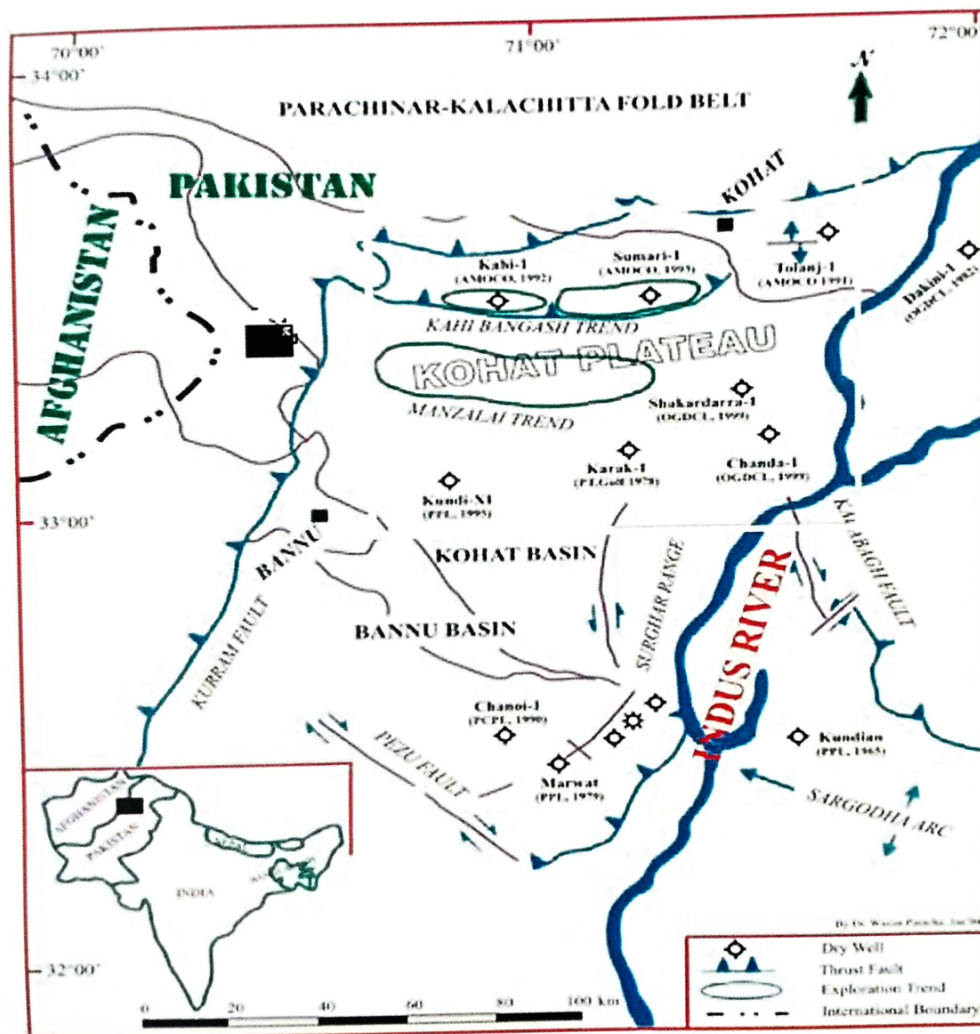


Figure 2.1: Tectonic map of study area (Kazmi, 1997)

2.2 Generalized Stratigraphy of Upper Indus Basin

ERA	AGE		UPPER INDUS BASIN		
	Period	Epoch	Potwar	Kohat	
Cenozoic	Quaternary	Pleistocene	Lei Conglomerates		
	Tertiary	Pliocene	Siwaliks Group	Soan	
				Dhok Pathan	
		Miocene	Rawalpindi Group	Nagri	
				Chinji	
		Oligocene		Kamlial	
				Murree	
Eocene	Chharat Group		Kohat		
			Kuldana		
Paleocene		Chorgali	Jatta Gypsum		
		Sakessar	Shekhan		
		Nammal	Panoba		
			Bahadur		
			Khel Salt		
			Patala		
			Lokhart		
			Hangu		
Mesozoic	Cretaceous	Late		Kawagarh	
		Early		Lumshiwal	
	Jurassic	Late		?	
		Middle		Samana Suk	
		Early		Datta	
	Triassic	Late		Kingriali	
		Middle			
	Early	Tredian			
		Mianwali			
Paleozoic	Permian	Late	Zaluch Group	Chhidru	
				Wargal	
	Early	Nilawahan Group		Amb	
				Sardhai	
			Warcha		
			Dandot		
			Tobra		
	Carboniferous to Ordovician				
Cambrian	Late		Baghanwala	Khisor	
	Middle	Jhelum Group	Juttana		
	Early		Kussak		
			Khewra		
Pre-Cambrian			Salt Range		
			Crystalline Basement		

Figure 2.2: Generalized stratigraphy of Upper Indus Basin, Pakistan (Qaudri, 1999)

2.3 Borehole well stratigraphy

Table 1.1: Borehole stratigraphy of well Manzalai-01

Age		Formations	Formation top (m)	Thickness (m)
Tertiary	Miocene	Murree Formation	16	1335
	Eocene	Kohat Formation	1351	186
	Eocene	Kuldana Formation	1537	1991
	Paleocene	Lockhart Limestone	3528	159
	Paleocene	Hangu Formation	3687	15
Cretaceous	Late	Kawagarh Formation	3702	195
	Early	Lumshiwai Formation	3897	63
		Chichali Formation	3960	184
Jurassic	Middle	Samana Suk Formation	4144	191
		Shinawari Formation	4335	176
	Early	Datta Formation	4511	64

2.4 Petroleum play

Table 1.2: Petroleum play of well Manzalai-01

Seal/Cap Rock	Lumshiwai Formation Kuldana Formation	Cretaceous Eocene
Reservoir Rock	Lumshiwai Formation Lockhart Limestone	Cretaceous Paleocene
Source Rock	Chichali Formation Hungu Formation	Cretaceous Paleocene

CHAPTER 3

PETROPHYSICAL ANALYSIS

3.1 Introduction

The assessment of the types of rock as well as their contact to fluids is considered as petro-physics. In symbolic definition, the word “Petra” pertains to “Rock” and “Physics” refers to the “Study of nature”. Consequently, the assessment of physicochemical geological formations as well as their ability to interact with fluids includes petro-physical study. Laboratory as well as log data will acquire petro-physical data. By studying and analyzing, well log findings by methodologies that are positioned in the borehole whether by taking sediment cores, petro-physicists sample source rock or reservoir.

For the area of relevance, the shale volume, clean volume, porosity, water saturation and hydrocarbon saturation are evaluated by measuring the hydrocarbon potential. By monitoring the water saturation and hydrocarbon saturation after because, the primary priority is to evaluate or accurately measure the hydrocarbon potential in the reservoir. Hydrocarbon saturation means how often rock pores have been saturated by hydrocarbon.

3.2 Steps for Petro-physical Analysis

The petro-physical research steps were taken as stated below:

- i. Volume of shale (V_{sh})
- ii. Porosity calculation (Φ)
- iii. Water resistivity (R_w)
- iv. Water saturation (S_w)
- v. Hydrocarbon saturation (S_H)

3.3 Methodology

The first and main task with proactively monitor of well Manzalai-01 have become effective regulation of logs by carrying log readings at multiple points, measuring different petro-physical boundary conditions. For the investigation of well

Manzalai-01, numerous strategies have been used to evaluate water as well as hydrocarbon saturation, relocating hydrocarbons or permeability from diverse log data.

3.3.1 Zone of Interest

The area of the formation serving as a potential reservoir is referred to as the zone of Interest. It varies from a few meters to tens of meters, depending on the formation. Mostly on ground of the gamma ray, caliper, neutron, density as well as resistivity logs, the zone of interest is defined. The requirements for marking an interest zone are as follows:

- i. The whole first condition is that the caliper should be constant, in other words that the bit size must not change significantly.
- ii. The second criterion would be that the GR ought to be minimal, implying that there is less shale content in lithology so it is clean.
- iii. The third criterion is that the log curve of resistivity should be available in the following triplicate:
MSFL is supposed to be lower than LLS and LLS is supposed to be lower than LLD
- iv. The fourth requirement is that the Neutron-Density crossover should cross and be at the lower values i.e, to step towards low values and each other.
- v. The fifth criterion is to search for the negative deflection of the SP that reveals about the permeability.

3.3.2 Calculations of Volume of Shale

The gamma ray has been used to test the shale content present in the formation. The higher shale content would have been the gamma ray value, that further means dirty formation. Formations which produce less radiation with a low amount of shale or clay content are identified as clean zones. The shale volume is measured with the aid of the following equation: $I_{GR} - V_{sh}$ (Schlumberger, 1974).

$$I_{GR} = (GR_{log} - GR_{min}) / (GR_{max} - GR_{min})$$

Where

I_{GR} = Index Gamma Ray.

GR log = The value of the gamma rays in the interest zone.

GR min = Values of minimum Gamma Rays.

GR max = Values of maximum Gamma Rays.

3.3.3 Volume of Clean

To measure the volume of clean, the following equation is used (Schlumberger, 1974):

$$V_{\text{clean}} = 1 - V_{\text{sh}}$$

Where

V_{sh} indicates volume of shale.

3.3.4 Porosity analysis and Calculations

Porosity is a physical characteristic of a rock which determines the state of total number of vacant rock spaces. It is known as the proportion in the percentage of the volume of pores that can contain fluids inside the rock. The two porosity groups are primary, i.e. that would be produced during rock deposition whereas secondary porosity i.e, that would be generated after deposition attributable to rock fracturing as well as dissolution (Tiab and Donaldson, 2015).

3.3.4.1 Density Porosity

The density value is computed using the density log density and thus the subsequent formula is used for a porosity calculation:

$$\Phi = (P_{\text{matrix}} - P_{\text{bulk}}) / (P_{\text{matrix}} - P_{\text{fluid}})$$

Here

P_{matrix} = Density of matrix (Limestone or Sandstone = 2.71/2.65 g/cm³)

P_{bulk} = Bulk density of the formation

P_{fluid} = Density of fluid (saline water = 1.1 g/cm³)

$$\text{PhiE} = \text{PhiA} * \text{V clean}$$

Where

PhiE = Effective porosity

PhiA = Average porosity

Vclean = Volume of clean

3.3.4.6 Resistivity of water

Water resistivity is crucial for the measurement of water saturation. The phases in which resistivity is measured are below:

Phase I

The first and foremost step is the Geothermal Gradient measurement, and it can be calculated by the help of equation stated below:

$$\text{Geothermal Gradient} = (\text{Borehole Temperature} - \text{Surface Temperature}) / \text{Total Depth}$$

Phase II

The next stage is to evaluate the temperature of the formation that can be measured by using given equations.

$$\text{Formation temperature} = (\text{Formation Top} * \text{Geothermal Gradient}) + \text{Surface Temperature}$$

Phase III

Rmf at Surface temperature is transformed to Rmf at Temperature of formation by using the chart GEN-9.

Phase IV

Rmf would then be converted to Rmfeq at the formation temperature using the SP-2 plot.

Phase V

The next phase seems to be using the SP Log to measure SSP. It is important for the estimation of $R_{w_{eq}}$. A straight line should be drawn going through all the $R_{mf_{eq}}$ that

$$\text{PhiE} = \text{PhiA} * \text{V clean}$$

Where

PhiE = Effective porosity

PhiA = Average porosity

Vclean = Volume of clean

3.3.4.6 Resistivity of water

Water resistivity is crucial for the measurement of water saturation. The phases in which resistivity is measured are below:

Phase I

The first and foremost step is the Geothermal Gradient measurement, and it can be calculated by the help of equation stated below:

$$\text{Geothermal Gradient} = (\text{Borehole Temperature} - \text{Surface Temperature}) / \text{Total Depth}$$

Phase II

The next stage is to evaluate the temperature of the formation that can be measured by using given equations.

$$\text{Formation temperature} = (\text{Formation Top} * \text{Geothermal Gradient}) + \text{Surface Temperature}$$

Phase III

Rmf at Surface temperature is transformed to Rmf at Temperature of formation by using the chart GEN-9.

Phase IV

Rmf would then be converted to Rmfeq at the formation temperature using the SP-2 plot.

Phase V

The next phase seems to be using the SP Log to measure SSP. It is important for the estimation of $R_{w_{eq}}$. A straight line should be drawn going through all the R_{mfeq} that

allows the $R_{w_{eq}}$ value, and used the SSP, Formation Temperature and thus the $R_{mf_{eq}}$ value in the SP-1 plots.

Phase VI

It is the last step in the measurement of water resistivity using SP-2 plot. The value of $R_{w_{eq}}$ for the calculation of R_w is often used.

3.3.4.7 Water saturation

Water saturation seems to be the sum of wet zone existing in the formation that would be known as the volume of water to pore-volume ratio. While using the Archie's formula, we measured water saturation.

$$S_w = \text{Square root } (R_w/R_t * (\text{Phi}E^2))$$

Where

R_w = Resistivity of water

R_t = Resistivity of true zone (calculated from LLD)

$\text{Phi}E$ = Effective porosity

3.3.4.8 Hydrocarbon saturation

R_w is needed to measure hydrocarbon saturation. The following equation calculates the saturation of hydrocarbons (Schlumberger, 1989).

$$S_H = 1 - S_w$$

Here

S_H = Saturation of Hydrocarbons

S_w = Saturation of Water

3.4 Petro-physical interpretation of well Mazalai-01

3.4.1 Zone of interests

Different areas of interest in both clastic and non-clastic reservoirs were classified in Manzalai-01. Lockhart Formation as well as Lumshiwai Formation in Manzalai-01 well is intended to be prospective reservoirs. Within these reservoir rocks, table 3.1 shows the thickness of each prospect zone.

Table 2.1: Showing the Potential Reservoirs of well Manzalai-01, zones and thickness of the formations

Formation	Zone of interest	Starting depth (m)	Ending depth (m)	Thickness (m)
Lockhart	Zone A	3556	3560	4
Lumshiwai	Zone B	3897	3917	20

3.4.2 Petro-physical analysis of Lockhart formation in well Manzalai-01

As the GR curve on track 1 has lower and consistent values as shown in figure 3.1, Manzalai-01 has clean lithology as well as the log patterns of Zone A, marked within Lockhart Limestone. A borehole is marginally over gauged, however borehole conditions are fine as track 1 of the caliper log is shown in the figure. In track 2, there is indeed a clear distinction among MSFL versus LLD, indicating the existence of fluid for formation. There is indeed a neutron density crossover that suggests a decline in the neutron as well as density values of the target region in the context of hydrocarbon. The lithology of Lockhart limestone is majorly composed of carbonates so it displaying the linear trend of sonic log.

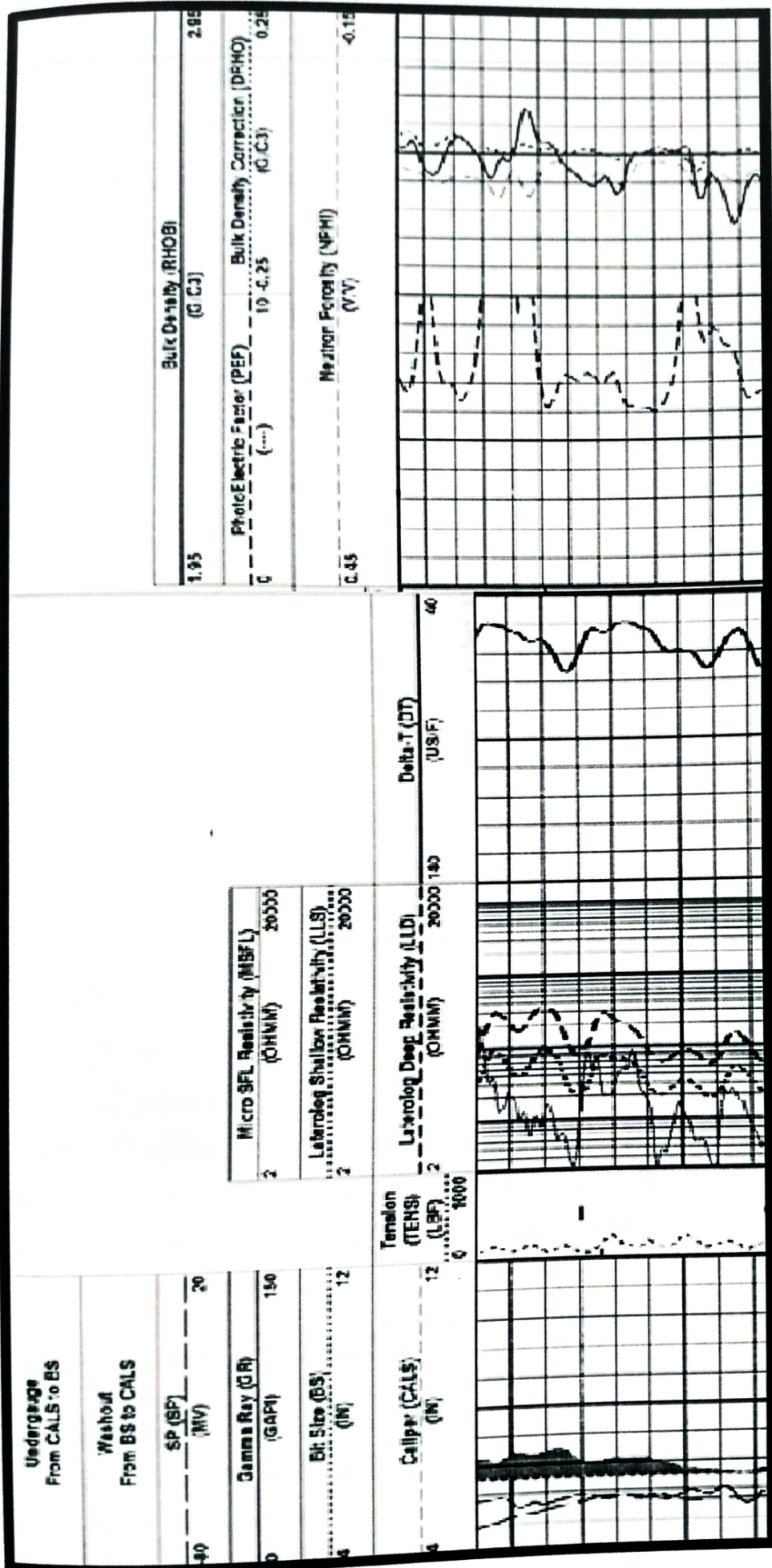


Figure 3.1: Log trends of Zone A, marked within Lockhart Limestone in well Manzalai-01

3.4.2.1 Volume of shale (Vsh) of zone of interest within Lockhart formation

The shale volume (Vsh) is referred to as the index of the gamma ray (IGR), which is the measurement of shale/clay consistency or lithological cleanliness. A shale volume spike implies a rise in gamma-ray, indicating radioactive formation, whereas clean lithology has less shale volume, shown by a decrease in gamma-ray values.

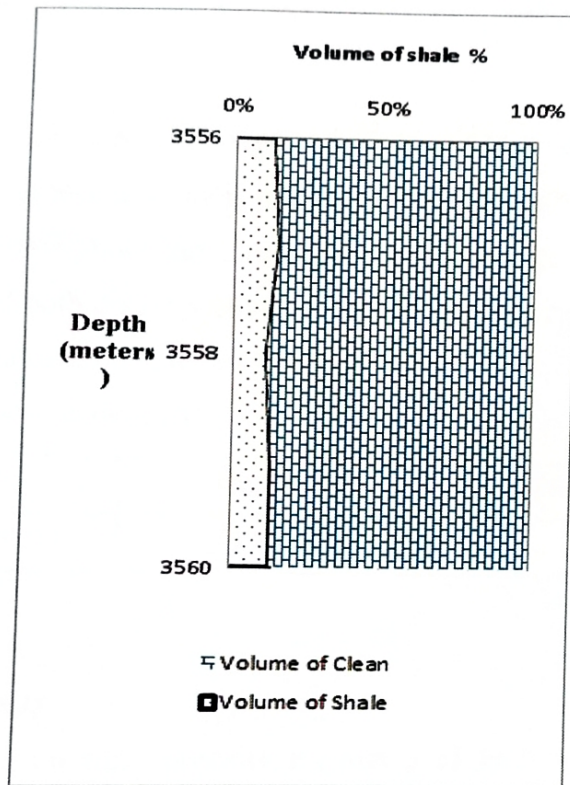


Figure 3.2: Relationship between volume of shale and volume of clean

The cross plot between shale volume and clean volume in the Lockhart formation (Zone A) is shown in figure 3.2, beginning at 3556 m depth and ending at 3560 m depth. From Figure 3.2, it is evident that shale volume shows low percentage values within the interest region. The volume of shale has a linear pattern at the start and the end of the zone of interest.

3.4.2.2 Calculation of porosities of zone of interest within Lockhart formation

I. Neutron Porosity

For calculating the fluid-filled porosity of the zone of interest, a neutron log is used. Neutron log direct informs you that in the API unit, porosity has values. The

average neutron porosity percentage is 2.2 % shown in table 3.2, while the neutron curve marked in zone of interest is showing decrease in values.

Table 3.2: Average neutron porosity (%)

Formation	Depth (m)	Average Neutron Porosity (%)
Lockhart (Zone A)	3556-3560	2.2

II. Density Porosity

A density log is used to provide us with knowledge on lithology and its distinct features, e.g, the presence of organic matter including porosity. It tests the formation's bulk density. In zone A, Lockhart Limestone's gross average porosity is 3.22 percent. In the initial depths of both the respective formation, the density porosity is greater, since there is very low value around depth 3559

Table 3.3: Average density porosity (%)

Formation	Depth (m)	Average Density Porosity (%)
Lockhart (Zone A)	3556-3560	3.22

III. Sonic Porosity

To determine the sonic porosity, the matrix of the lithology as well as transit time is required.

Table 3.4: Average sonic porosity

Formation	Depth (m)	Average Sonic Porosity (%)
Lockhart (Zone A)	3556-3560	6.81

IV. Average Porosity

It can be determined by taking the neutron average and thus the porosity of density.

Table 3.5: Average porosity

Formation	Depth (m)	Average Porosity (%)
Lockhart (Zone A)	3556-3560	2.71

V. Effective Porosity

Effective porosity is the amount of pores that are interconnected or have interconnected pores found in a rock. Often, effective porosity is less than total porosity. Because it represents how much fluid is going to move, successful porosity matters. This equation calculates effective porosity if sonic porosity is not available.

Table 3.6: Average effective porosity of Lockhart Formation

Formation	Depth (m)	Average Effective Porosity (%)
Lockhart (Zone A)	3556-3560	2.3

3.4.2.3 Relationship between V_{shale} and Porosities

Neutron porosity means total porosity, but because efficient porosity is always smaller than total porosity, effective porosity is higher than that as shown in figure 3.3.

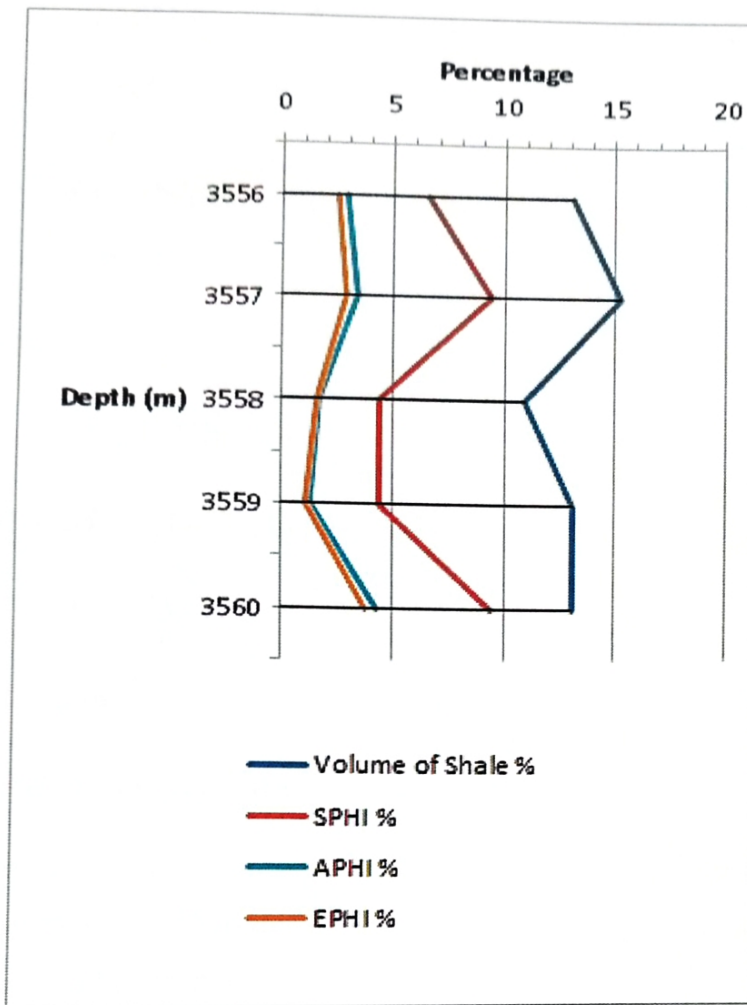


Figure 3.3: Variation in PhiS, PhiA and PhiE

3.4.2.4 Resistivity of Water of zone of interest within Lockhart Formation

It is the key and perhaps most sensitive approach to the measurement of water saturation including hydrocarbon saturation assessment from water saturation. High water saturation and lower hydrocarbon saturation will be activated if the water resistivity is high, and vice versa. The resistivity of water can be calculated by two methods, which are:

I. Method of SP

II. Method for apparent resistivity (R_w)

The most effective technique is the SP method, as well as the least accurate method used to determine water resistivity is Apparent R_w . So, the SP method has been

used here to measure water resistivity. The SP process requires a total of seven steps which are accompanied by conducting measurements. Geothermal gradient of well

Where,

I. Geothermal gradient

$$\text{BHT} = 115^{\circ}\text{C}$$

$$\text{S.T} = 29^{\circ}\text{C}$$

$$\text{Total Depth} = 4575\text{m}$$

$$= \text{BHT} - \text{ST} / \text{Total Depth}$$

$$= 115 - 29 / 4575$$

$$= 0.018^{\circ}\text{C/m}$$

II. Formation Temperature

Where,

$$\text{Formation Top} = 3556 \text{ m}$$

$$\text{Geothermal Gradient} = 0.018^{\circ}\text{C/m}$$

$$= (\text{Formation top} * \text{Geothermal Gradient}) + \text{Surface Temperature}$$

$$= (3556 * 0.018) + 29$$

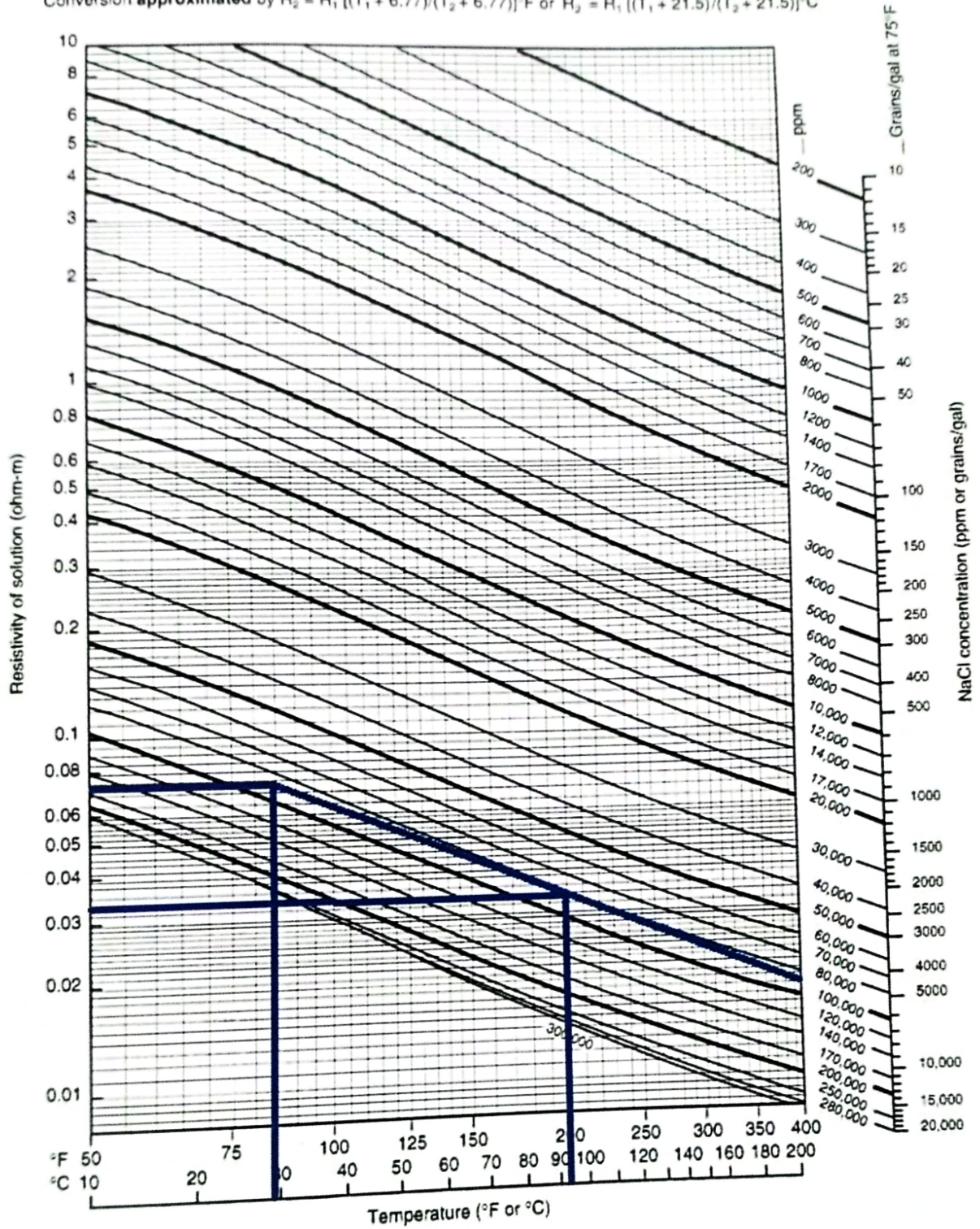
$$= 93^{\circ}\text{C}$$

III. Rmf at Surface Temperature to Rmf at Formation temperature

By using Gen-09 chart,

$$0.075 \text{ ohm-m} - 0.034 \text{ ohm-m}$$

Conversion approximated by $R_2 = R_1 [(T_1 + 6.77)/(T_2 + 6.77)]^F$ or $R_2 = R_1 [(T_1 + 21.5)/(T_2 + 21.5)]^C$



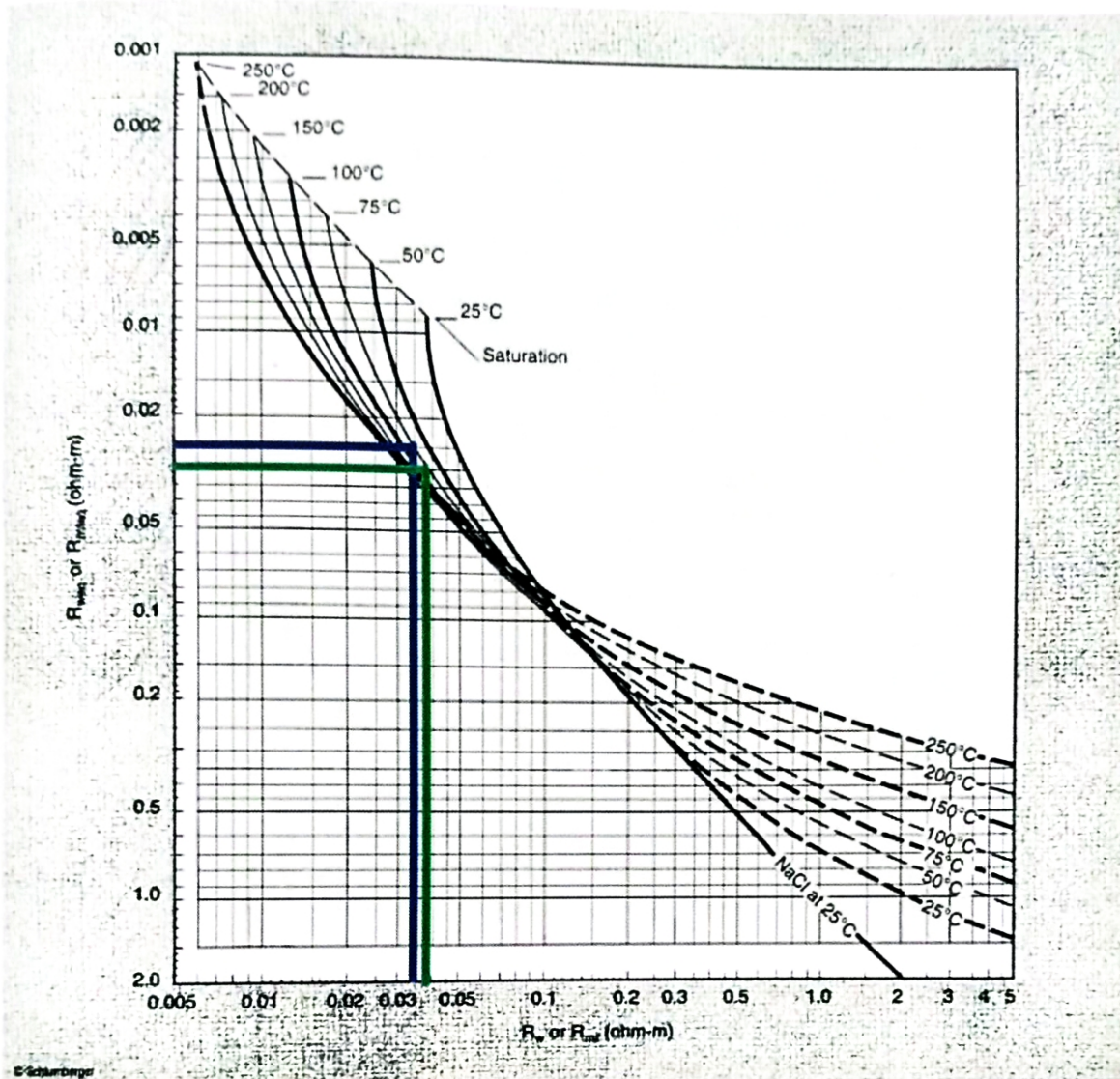
© Schlumberger

Figure 3.4: Gen-9 chart to convert Rmf (from Surface temperature to Formation temperature)

IV. Rmf to Rmf_{eq}

Using SP-2 metric chart

0.034 ohm-m - 0.025 ohm-m



SP

Figure 3.5: SP-2m metric chart for conversion of R_{mf} to R_{mfeq}

V. Calculation of Static Spontaneous Potential by using SP log

$SSP = +10$

VI. SSP and $R_{mf_{eq}}$ to $R_{w_{eq}}$

Using SP-1 chart

$+10 \text{ \& } 0.025 \text{ ohm-m} - 0.03 \text{ ohm-m}$

R_weq Determination from E_{SSP}
Clean formations

SP-1

This chart and nomograph calculate the equivalent formation water resistivity, R_weq, from the static spontaneous potential, E_{SSP}, measurement in clean formations.

Enter the nomograph with E_{SSP} in mV, turning through the reservoir temperature in °F or °C to define the R_{mf}/R_w ratio. From this value, pass through the R_{mf} value to define R_weq.

For predominantly NaCl muds, determine R_{mf} as follows:

- If R_{mf} at 75°F (24°C) is greater than 0.1 ohm-m, correct R_{mf} to formation temperature using Chart Gen-9, and use R_{mf} = 0.85 R_{mf}.
- If R_{mf} at 75°F (24°C) is less than 0.1 ohm-m, use Chart SP-2 to derive a value of R_{mf} at formation temperature.

Example: SSP = 100 mV at 250°F

R_{mf} = 0.70 ohm-m at 100°F
or 0.33 ohm-m at 250°F

Therefore, R_{mf} = 0.85 × 0.33

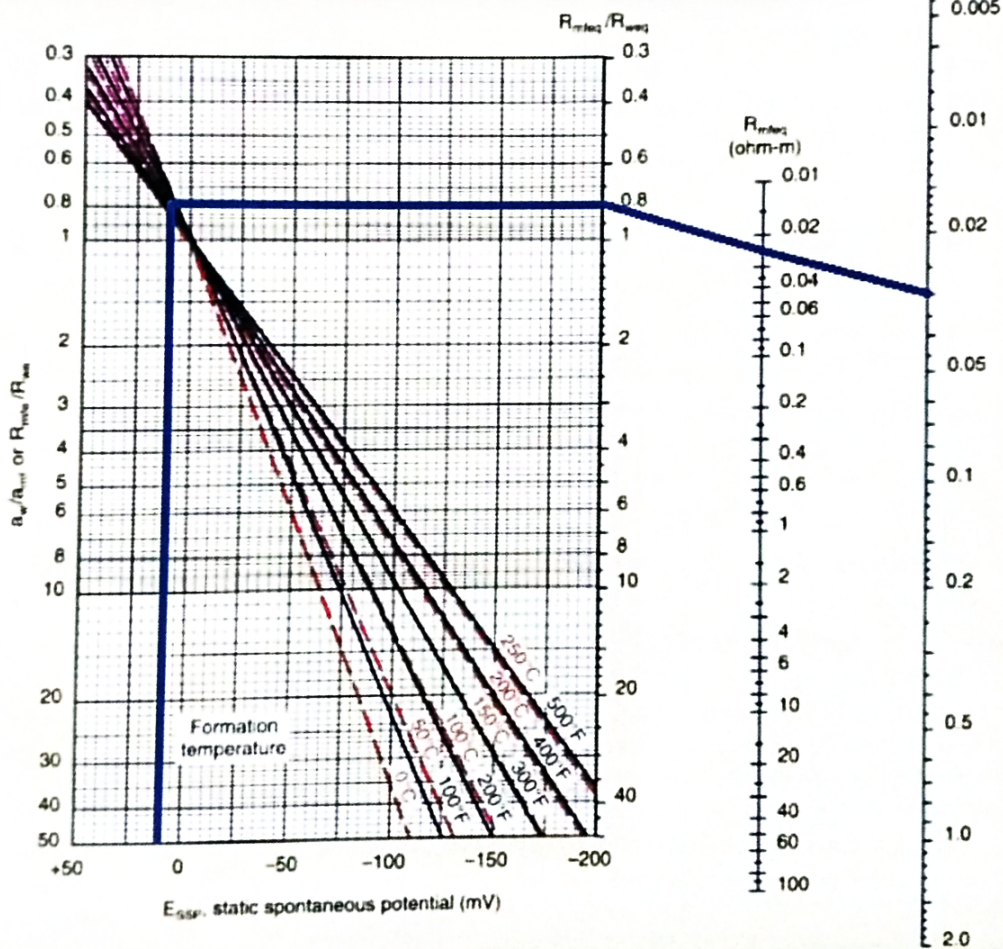
= 0.28 ohm-m at 250°F

R_weq = 0.025 ohm-m at 250°F

E_{SSP} = -K_c log(R_{mf}/R_weq)

K_c = 61 + 0.133 T_F

K_c = 65 + 0.24 T_C



© Schlumberger

2-5

Figure 3.6: SP-1 chart for conversion of R_{mf} to R_weq

VII. R_weq to R_w

Using SP-2 metric chart (fig. 3.5)



0.03 ohm-m - 0.039 ohm-m

3.4.2.5 Saturation of water and Saturation of hydrocarbon in zone of interest within Lockhart formation:

The water saturation gives information about the number of pore spaces, water filled. Water saturation will determine hydrocarbon saturation. The Fig.3.7 shows the cross plot among saturation of water as well as saturation of hydrocarbons at the target depth of the region of interest, spanning from 3556 m to 3560 m. At the sustained increase, hydrocarbon saturation and water saturation were roughly equal, yet water saturation increased with the rise in depth. The highest saturation value for hydrocarbons, at a depth of 3558 m, is 94.7%.

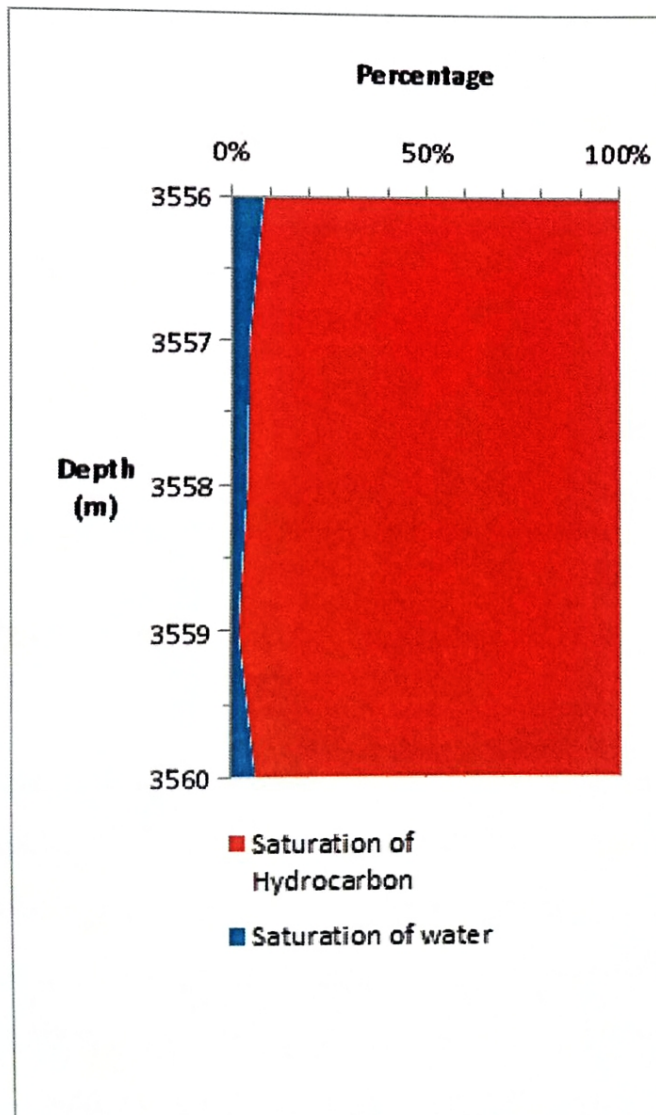


Figure 3.7: Variation in water saturation and hydrocarbon saturation within marked zone of interest

3.4.2.6 Results

Table 3.7: Results of petro-physical analysis of Lockhart Formation of well Manzalai-01

Formation	Lockhart
Zone	A
Thickness(m)	4
Average volume of shale (%)	13
Average volume of clean (%)	87
Average Total Porosity (%)	2.71
Average Effective porosity (%)	2.35
Resistivity of water (Ω m)	0.039
Average Water saturation (%)	5.2
Average Hydrocarbon saturation (%)	94.7

3.4.3 Petro-physical analysis of Lumshiwai Formation in well Manzalai-01

As the Gamma-ray curve in track 1 has inconsistent and low values, this formation has dirty lithology in Manzalai-01, as shown in fig 3.8. The borehole is under-gauged, however the optimal borehole conditions are good. In Track 2, there is a clear difference between MSFL and LLD, as MSFL is less than LLD, indicating that fluid formation is present. As the neutron and density values are declining, there is a neutron density crossover that suggests hydrocarbon presence. The formation of

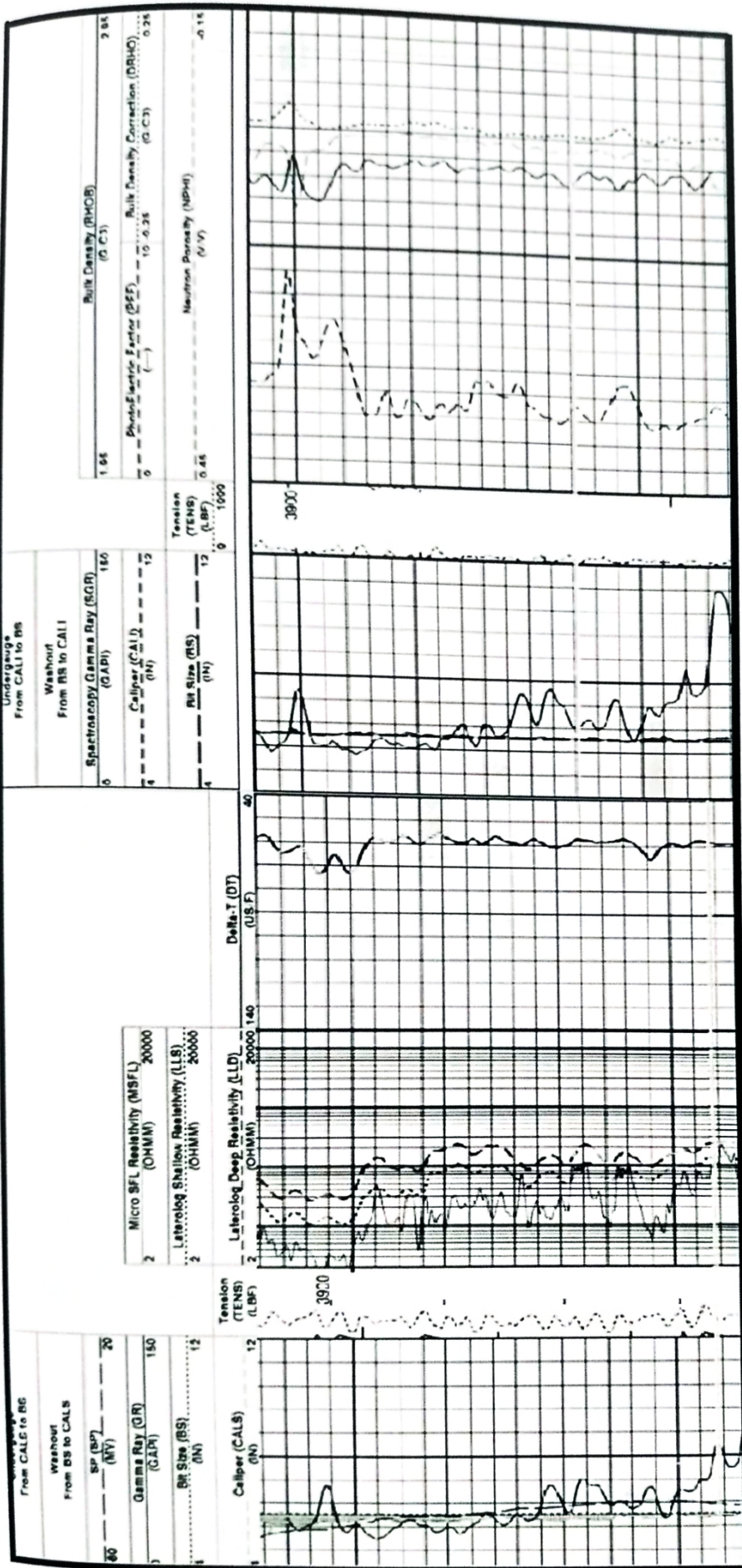


Figure 3.8: Log trends of Zone B, marked within Lumshiwai Formation in well Manzalai-01

lumshiwai is primarily composed of sandstone, so it does not indicate a linear sonic log trend.

3.4.3.1 Volume of shale (Vsh) in the zone of interest of Lumshiwai Formation

The shale volume (Vsh) is attributed as the index of the gamma ray (IGR), which is the measurement of shale/clay consistency or simply lithological cleanliness. A spike in shale volume implies an increase in gamma-ray, suggesting radioactive formation, whilst clean lithology has lower shale volume, reflecting a decrease in gamma-ray concentrations shown in figure 3.9.

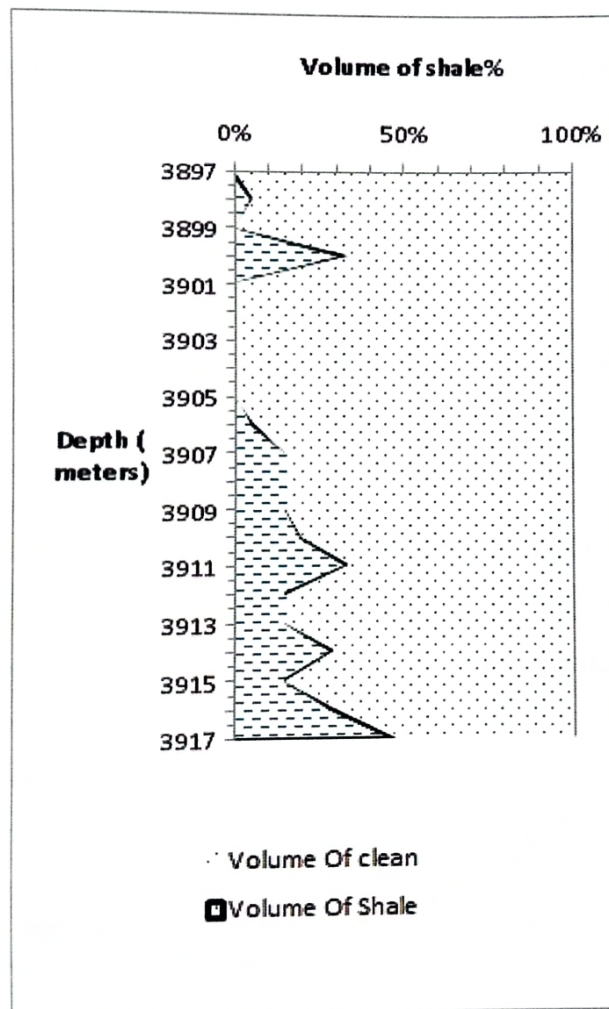


Figure 3.9: Relationship between Vshale and Vclean

A cross plot amongst shale volume and clean volume in the interest zone beginning at depth 3897 m while ending at depth 3917 m in the Lumshiwai Formation is shown in figure 3.9. It is evident from the figure that shale volume demonstrates low

percentage values within the interest region. The quantity of shale within the interest zone varies (Zone B). The shale volume is very low at the beginning and elevated at the end. There is an abrupt rise and decrease in Vsh values which further leads to higher values throughout the Lumshiwai Formation till the end of that scale within this particular field of interest.

3.4.3.2 Calculations of porosities in the zone of interest of Lumshiwai Formation

I. Neutron Porosity

For calculating the fluid-filled porosity of the region of interest, a neutron log has been used. Neutron log direct notifies that porosity has values in the API unit. The average percentage of neutron porosity is 2.85 percent, although the neutron curve marked in the interest zone indicates decreases in values in figure 3.8.

Table 3.8: Average neutron porosity

Formation	Depth (m)	Average Neutron Porosity (%)
Lumshiwai (Zone B)	3897-3917	2.85

II. Density Porosity

A density log is used to provide us with knowledge on lithology and its distinct features e.g, the presence of organic matter including porosity. It tests the formation's bulk density. In zone B, Lumshiwai formation gross average density porosity is 1.90 percent.

Table 3.9: Average density porosity

Formation	Depth (m)	Average Density Porosity (%)
Lumshiwai (Zone B)	3897-3917	1.90

III. Sonic Porosity

To determine the sonic porosity, the matrix of the lithology as well as transit time is required.

Table 3.10: Average sonic porosity

Formation	Depth (m)	Average Sonic Porosity (%)
Lumshiwai (Zone B)	3897-3917	3.88

IV. Average Porosity

It can be determined by taking the neutron average and thus the porosity of density.

Table 3.11: Average porosity

Formation	Depth (m)	Average Porosity (%)
Lumshiwai (Zone B)	3897-3917	2.38

V. Effective Porosity

It is the interconnected amount of pores found in a rock. Efficient porosity is always inferior to maximum porosity. Mainly because it represents how much fluid is going to move, successful porosity matters.

Table 3.12: Average effective porosity

Formation	Depth (m)	Average Effective Porosity (%)
Lumshiwai (Zone B)	3897-3917	2.06

3.4.3.3 Relationship between Vshale and porosities

The volume of shale and porosities are shown in Figure 3.9, with their interaction with each other. Complete porosity is indicated by neutron porosity and is indicated by higher than effective porosity, which is mostly below total porosity. At the beginning and end of formation, the shale volume percentage is higher. In the center of the zone of interest, neutron porosity increases, where shale volume decreases, while effective porosity increases as well.

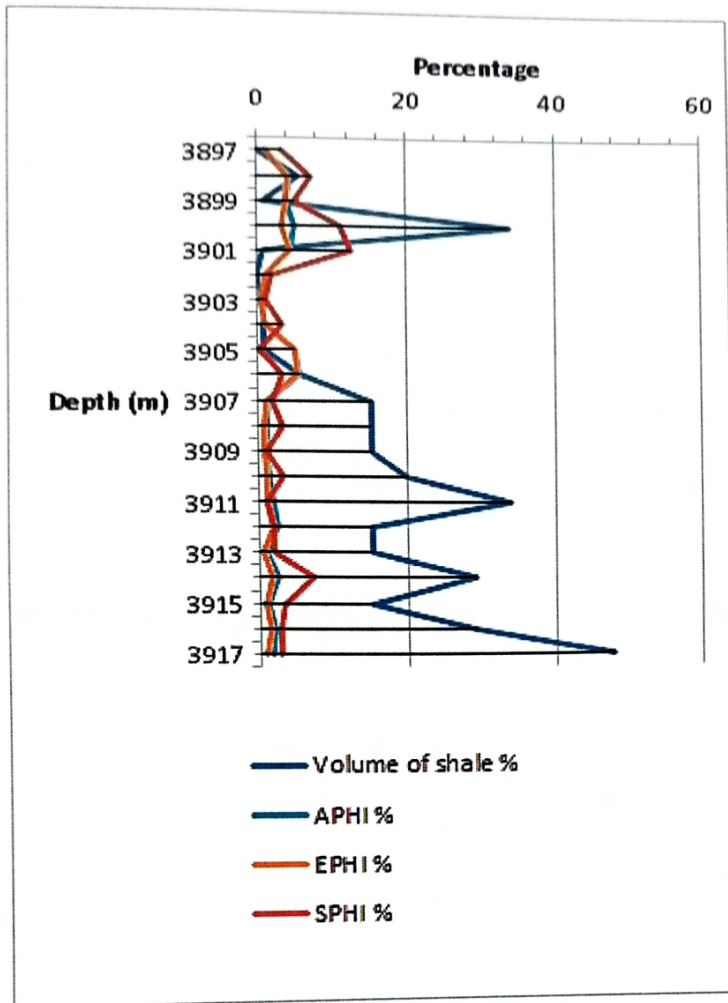


Figure 3.10: Relationship between Vshale and porosities

3.4.3.4 Resistivity of water of zone of interest within Lumshiwal Formation

The best approach is the SP method, obvious R_w is the least reliable method for determining water resistivity. The SP method was used for water resistivity calculation here. A total of seven steps accompanying measurement are needed in the SP process.

I. Geothermal gradient of well:

Where,

$$BHT = 115^{\circ}C$$

$$S.T = 29^{\circ}C$$

$$\text{Total Depth} = 4575m$$

$$= \frac{BHT - ST}{\text{Total Depth}}$$

$$= 115 - 29 / 4575$$

$$= 0.018^{\circ}\text{C/m}$$

II. Formation temperature:

Where,

$$\text{Formation Top} = 3897\text{m}$$

$$\text{Geothermal Gradient} = 0.018^{\circ}\text{C/m}$$

$$= (\text{Formation top} * \text{Geothermal Gradient}) + \text{Surface Temperature}$$

$$= (3897 * 0.018) + 29$$

$$= 99.14^{\circ}\text{C}$$

III. Rmf at Surface Temperature to Rmf at Formation Temperature:

Using Gen-9 chart

$$0.075 \text{ ohm-m} - 0.03 \text{ ohm-m}$$

Conversion approximated by $R_{fs} = R_f \left[\frac{T_s + 6.77}{T_f + 6.77} \right]^2$ or $R_{fs} = R_f \left[\frac{T_s + 21.5}{T_f + 21.5} \right]^2$

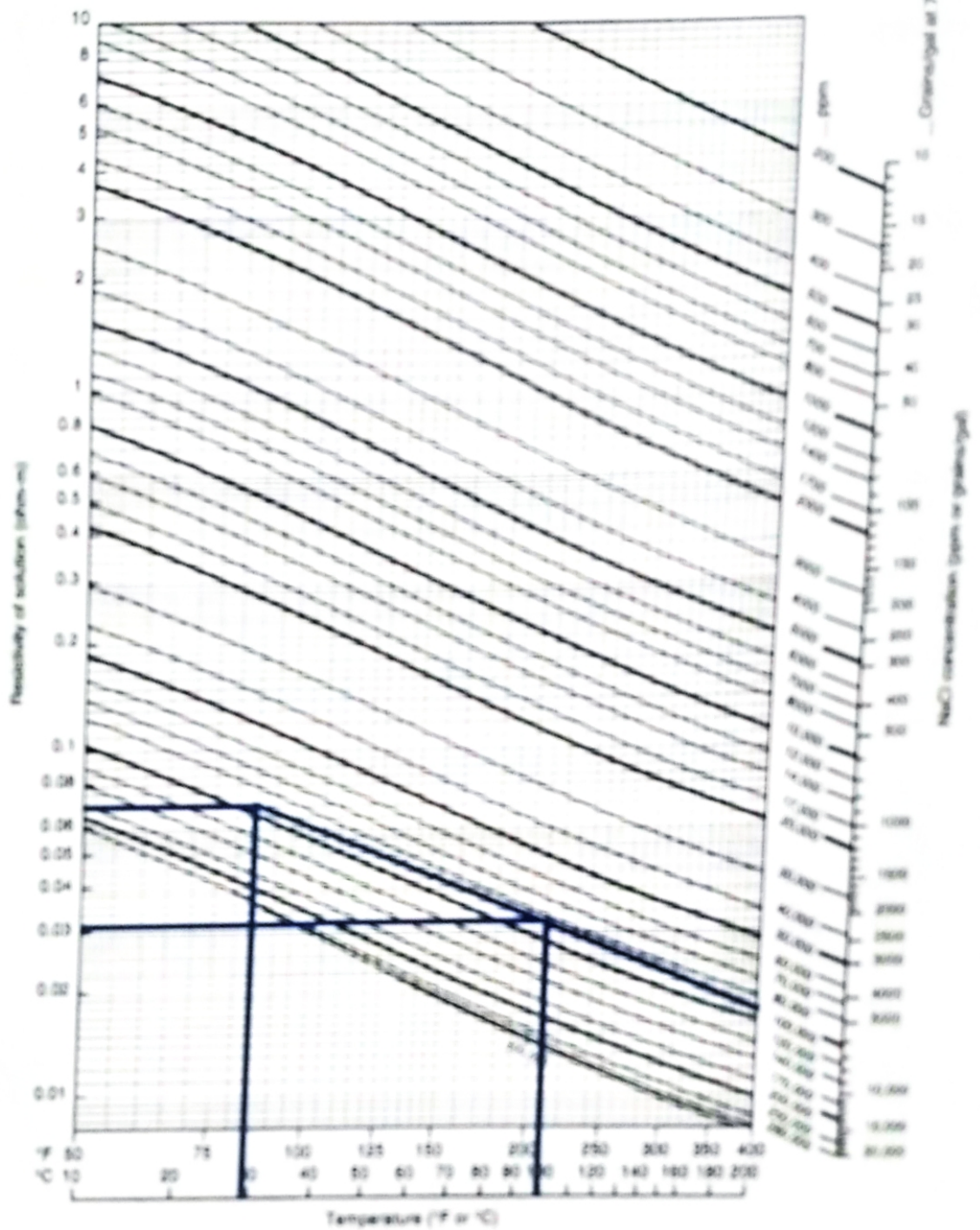


Figure 3.11: Gen-9 chart to convert R_{mf} at surface temperature to R_{mf} at formation temperature

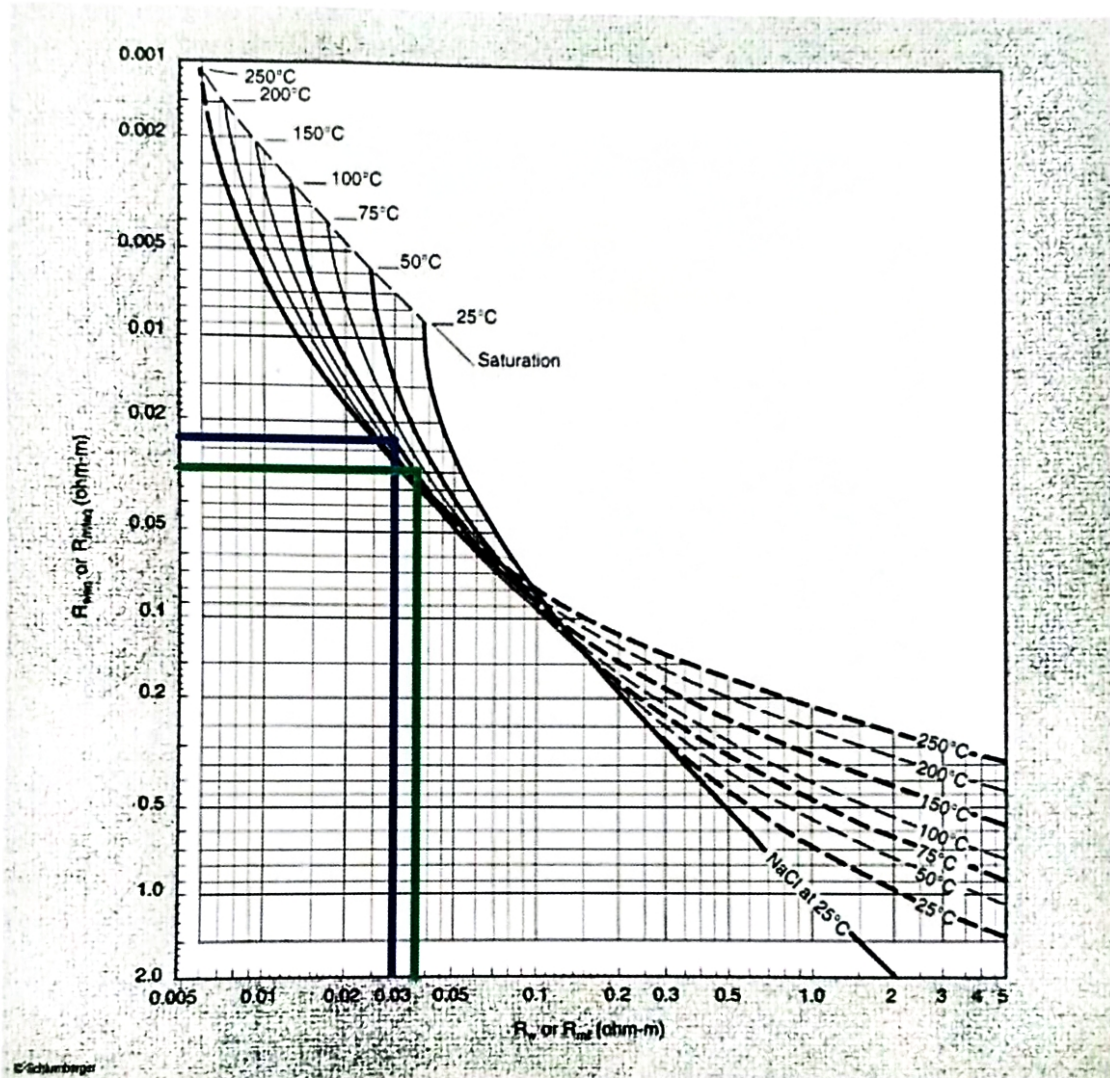
IV. R_{mf} to R_{mfq}

Using SP-2m metric chart

0.03 ohm-m - 0.025 ohm-m

R_w versus R_{weq} and Formation Temperature

SP-2m
(Metric)



SP

Figure 3.12: SP-2m metric chart to convert R_{mf} to $R_{mf_{eq}}$

V. Calculation of Static Spontaneous Potential using SP log

$$SSP = +10$$

VI. SSP and $R_{mf_{eq}}$ to $R_{w_{eq}}$

Using SP-1 chart

$$+10 \text{ \& } 0.025 \text{ ohm-m} - 0.03 \text{ ohm-m}$$

R_weq Determination from E_{SSP}
Clean formations

SP-1

This chart and nomograph calculate the equivalent formation water resistivity, R_weq, from the static spontaneous potential, E_{SSP}, measurement in clean formations.

Enter the nomograph with E_{SSP} in mV, turning through the reservoir temperature in °F or °C to define the R_{mfeq}/R_w ratio. From this value, pass through the R_{mfeq} value to define R_weq.

For predominantly NaCl muds, determine R_{mfeq} as follows:

- a. If R_{mfeq} at 75 °F (24 °C) is greater than 0.1 ohm-m, correct R_{mfeq} to formation temperature using Chart Gen-9, and use R_{mfeq} = 0.85 R_{mfeq}.
- b. If R_{mfeq} at 75 °F (24 °C) is less than 0.1 ohm-m, use Chart SP-2 to derive a value of R_{mfeq} at formation temperature.

Example: SSP = 100 mV at 250 °F

R_{mfeq} = 0.70 ohm-m at 100 °F
or 0.33 ohm-m at 250 °F

Therefore, R_{mfeq} = 0.85 × 0.33
= 0.28 ohm-m at 250 °F

R_weq = 0.025 ohm-m at 250 °F

E_{SSP} = -K_c log (R_{mfeq}/R_weq)

K_c = 61 + 0.133 T_F

K_c = 65 + 0.24 T_C

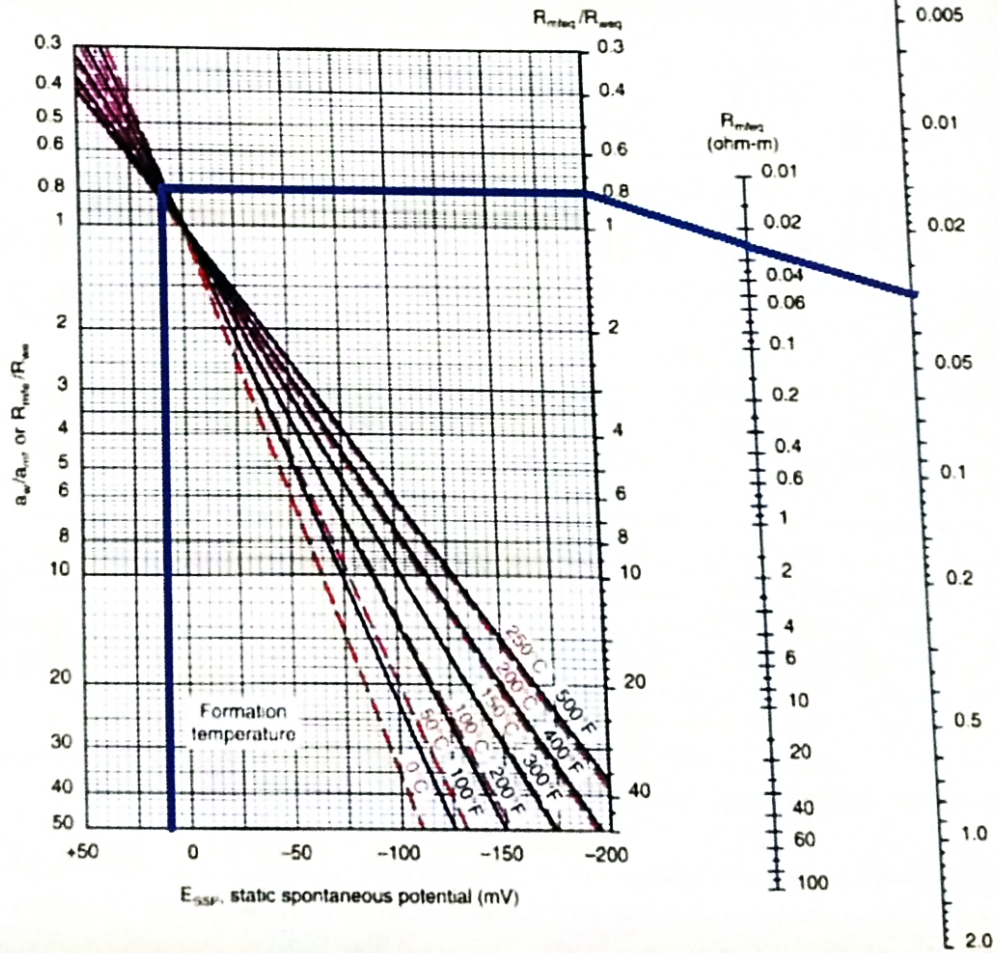


Figure 3.13: SP-1 chart to convert R_{mfeq} to R_weq

VII. $R_{w_{eq}}$ to R_w

Using SP-2m metric chart (fig. 3.12)

$$0.03 \text{ ohm-m} - 0.038 \text{ ohm-m}$$

3.4.3.5 Saturation of water and saturation of hydrocarbon of the zone of interest within Lumshiwai Formation

Water saturation informs you the amount of pore spaces filled with water. Hydrocarbon saturation can be determined by water saturation. For clean lithology, Archie's equation is being implied. Three equations are determined or measured by water saturation, which are as follows:

1. Archie's Equation
2. Indonesian Equation
3. Simandoux Equation

For clean lithology, Archie's equation is used, while for all rocks, Indonesian and Simandoux equations are used. Clean lithology is used in this field of interest, so Archie's is used to measure water saturation and the equation is:

$$S_w = \text{Square root } (R_w)/R_t * (EPHI)^2$$

Where

S_w = Saturation of water

R_w = Resistivity of water

R_t = Resistivity of true zone (calculated from LLD)

EPHI = Effective porosity

The number of pores that are filled with hydrocarbons represents the saturation of hydrocarbons. Water saturation and hydrocarbon saturation have an opposite relationship. Hydrocarbon saturation can be determined by means of the following equation:

$$S_H = 1 - S_w$$

Where

S_H = Saturation of hydrocarbons

S_W = Saturation of water

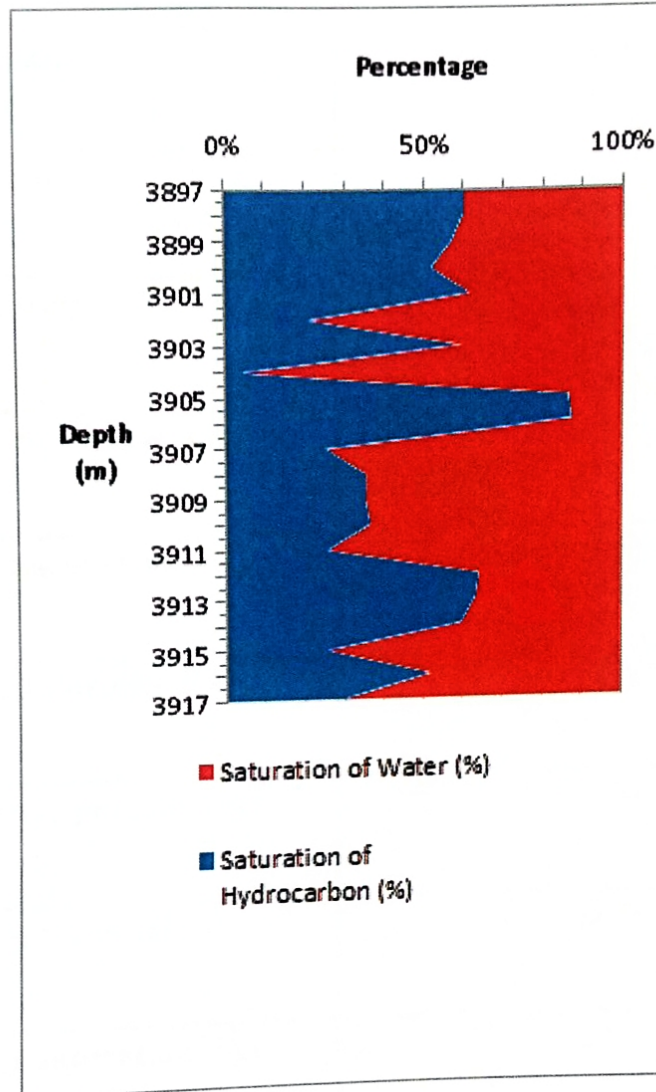


Figure 3.14: Variation in water saturation and hydrocarbon saturation within marked zone of interest

Fig.3.13 shows the cross plot regarding saturation of water as well as saturation of hydrocarbons at the target depth of the region of interest, varying from 3897 m to 3917 m. At the initial depth, the saturation of hydrocarbon and water is approximately equal, but water saturation increased as the depth increased. For hydrocarbons, the peak saturation value is from 3905 m to 3907 m in depth. It is evident from Fig 3.13 that there have been hydrocarbon areas in the region of interest, but this field is more water-saturated.

3.4.3.6 Results

Table 3.13: Results of petro-physical analysis of Lumshiwai formation of well Manzalai-01

Formation	Lumshiwai
Zone	B
Thickness(m)	20
Average volume of shale (%)	14.33
Average volume of clean (%)	85.66
Average Total Porosity (%)	2.38
Average Effective porosity (%)	2.06
Resistivity of water (Ω m)	0.038
Average Water saturation (%)	52.1
Average Hydrocarbon saturation (%)	47.83

CONCLUSION

On the basis of petro-physical analysis it is concluded that:

In well Manzalai-01, both clastic and carbonate reservoirs are present. On the basis of logs trends one zone of interest has been marked both in Lockhart and Lumshiwal formation. On the basis low percentage of Volume of Shale and the high percentage of the Hydrocarbons, the results computed from the petro-physical Analysis suggest that both Formations are acting as major Reservoirs in well Manzalai-01.

References

- Berecz, F. (2010). function of geological study in Pakistan hydrocarbon research. MOL scientific magazine, 114.
- Ibrahim, S. (2009). Stratigraphy of Pakistan, Islamabad: Geological survey of Pakistan.
- Jan, K. A. (1997). Geology and tectonics of Pakistan. researchgate, 45-47.
- Kazmi, J. (1997). Geology of pakistan, Karachi: Graphic publishers.
- Saleh, A. (2015). oil and gas sector of Pakistan and sustainable development. Deutchland: LAP Lambert Academic Publishing.

APPENDIX

Lockhart Formation												
Depth	Vshale	Vclean	PhiN %	PhiD %	PhiDT %	PhiA %	PhiE %	Rw	Sw %	Sh %		
3556	13.04348	86.95652	2	3.726708	6.52173913	2.863354	2.489873	0.039	8.516676	91.48332		
3557	15.21739	84.78261	3	3.726708	9.420289855	3.363354	2.851539	0.039	4.711516	95.28848		
3558	10.86957	89.13043	1	2.484472	4.347826087	1.742236	1.552863	0.039	4.336909	95.66309		
3559	13.04348	86.95652	2	0.621118	4.347826087	1.310559	1.139617	0.039	2.250562	97.74944		
3560	13.04348	86.95652	3	5.590062	9.420289855	4.295031	3.73481	0.039	6.596989	93.40301		
Lumshiwal Formation												
3897	0	1	1	1.212121	3.474903	1.106061	1.106061	0.038	39.9598	60.0402		
3898	5.660377	0.943396	3	6.060606	7.341577	4.530303	4.273871	0.038	41.63703	58.36297		
3899	0.943396	0.990566	2	6.060606	5.023184	4.030303	3.992281	0.038	44.57384	55.42616		
3900	33.96226	0.660377	10	0	11.20556	5	3.301887	0.038	49.89599	50.10401		
3901	0.943396	0.990566	3	6.060606	12.75116	4.530303	4.487564	0.038	39.65432	60.34568		
3902	0	1	1	1.212121	1.931994	1.106061	1.106061	0.038	82.17391	17.82609		
3903	0.943396	0.990566	1	0	1.159196	0.5	0.495283	0.038	39.9796	60.0204		
3904	0.943396	0.990566	1	1.212121	3.477589	1.106061	1.095626	0.038	99.46137	0.538627		
3905	0.943396	0.990566	10	0	0.386399	5	4.95283	0.038	13.91533	86.08467		
3906	5.660377	0.943396	10	1.212121	3.477589	5.606061	5.288736	0.038	13.03151	86.96849		
3907	15.09434	0.849057	1	1.818182	1.931994	1.409091	1.196398	0.038	77.67653	22.32347		
3908	15.09434	0.849057	1	1.212121	3.477589	1.106061	0.939108	0.038	64.45473	35.54527		
3909	15.09434	0.849057	1	1.212121	1.159196	1.106061	0.939108	0.038	64.5557	35.4443		
3910	19.81132	0.801887	2	0.606061	3.477589	1.30303	1.044883	0.038	65.95978	34.04022		
3911	33.96226	0.660377	2	1.818182	1.159196	1.909091	1.26072	0.038	77.31131	22.68869		
3912	15.09434	0.849057	2	3.030303	1.931994	2.515152	2.135506	0.038	37.26622	62.73378		
3913	15.09434	0.849057	1	0.606061	1.931994	0.80303	0.681818	0.038	36.7549	63.2451		
3914	29.24528	0.707547	2	3.030303	7.341577	2.515152	1.779588	0.038	42.00663	57.99337		
3915	15.09434	0.849057	1	1.212121	3.477589	1.106061	0.939108	0.038	77.35885	22.64115		
3916	29.24528	0.707547	2	1.818182	2.704791	1.909091	1.350772	0.038	49.79321	50.20679		
3917	48.11321	0.518868	3	0.606061	2.704791	1.80303	0.935535	0.038	73.66937	26.33063		





Petrophysical analysis of Well Manzalai-01, Upper Indus Basin, Pakistan

ORIGINALITY REPORT

5%

SIMILARITY INDEX

1%

INTERNET SOURCES

1%

PUBLICATIONS

4%

STUDENT PAPERS

PRIMARY SOURCES

- 1** Submitted to Higher Education Commission Pakistan
Student Paper 3%
- 2** nceg.upesh.edu.pk
Internet Source 1%
- 3** www.scribd.com
Internet Source <1%
- 4** Abdus Satter, Ghulam M. Iqbal. "Reservoir rock properties", Elsevier BV, 2016
Publication <1%
- 5** pt.scribd.com
Internet Source <1%
- 6** Asam Farid, Pervez Khalid, Muhammad Y. Ali, Muhammad Asim Iqbal, Khan Zaib Jadoon. "Seismic stratigraphy of the Mianwali and Bannu depressions, north-western Indus foreland basin", International Journal of Earth Sciences, 2017
Publication <1%

Exclude quotes On
Exclude bibliography Off

Exclude matches Off